ISSN 0021-8944, Journal of Applied Mechanics and Technical Physics, 2017, Vol. 58, No. 3, pp. 461–468. © Pleiades Publishing, Ltd., 2017.
Original Russian Text © V.A. Gorokhov, S.A. Kapustin, Yu.A. Churilov.

NUMERICAL SIMULATION OF PLASTIC DEFORMATION AND DAMAGE ACCUMULATION IN STRUCTURAL MATERIALS UNDER VARIOUS LOW-CYCLE LOADING CONDITIONS

V. A. Gorokhov, S. A. Kapustin, and Yu. A. Churilov

UDC 539.3

Abstract: This paper presents the results of a finite-element study of elastic-plastic deformation and damage accumulation in structural materials under various cyclic loading conditions. Material behavior is described by the relations of damage mechanics using thermoplastic model which takes into account the plastic deformation of material under cyclic loading and the kinetic equations of the energy theory of damage accumulation. The basic laws of plastic deformation and development of damage in materials under hard, soft, symmetric, and asymmetric low-cycle loading are established.

Keywords: plastic deformation, low-cycle loading, damage accumulation, numerical modeling.

DOI: 10.1134/S0021894417030117

INTRODUCTION

Problems of mathematical modeling of the elastic-plastic deformation of materials and structures under low-cycle fatigue are considered in [1–6]. These papers focus on the development of models describing low-cycle deformation and damage accumulation in structural materials under isothermal and nonisothermal loading [1–4] with additional hardening under proportional and disproportional cyclic loading [5] and the influence of the multi-stage nature of damage development on the fracture process [2, 3, 6]. In this paper, the kinetic laws of low-cycle plastic deformation and damage accumulation in structural materials for some low-cycle loading conditions (hard, soft, symmetric and asymmetric) are studied by numerical solution of the corresponding problems of thermoplasticity for structural members made of 12Kh18N10T stainless steel.

The problems are solved by the finite element method using the relations of damage mechanics, the plasticity model, and the kinetic equations of energy damage accumulation theory [2, 6]. The deformation process for individual loading cycles is divided into a number of stages with subsequent integration of incremental equations describing the state of the investigated structures with a consideration of the history of irreversible deformation and material damage accumulation.

The kinetics of low-cycle plastic deformation of structures is largely determined by the loading conditions at individual points of the material of the investigated structures.

For the low-cycle plastic deformation of structural members in a uniform stress-strain state, desired in corresponding experiments, a number of regimes can be distinguished, each of which is characterized by a particular

Research Institute for Mechanics of Lobachevsky National Research State University of Nizhny Novgorod, Nizhny Novgorod, 603950 Russia; vas-gor@rambler.ru, sergei.kapustin@mail.ru, chyuan@rambler.ru. Translated from Prikladnaya Mekhanika i Tekhnicheskaya Fizika, Vol. 58, No. 3, pp. 98–107, May–June, 2017. Original article submitted June 8, 2015; revision submitted July 11, 2016.

change in plastic strain, e.g., hard loading with a specified strain amplitude and soft loading with specified ranges of the stress tensor components.

From the results of experiments,it follows that for cyclically stable and cyclically hardening materials under hard symmetric and asymmetric loading, the coordinates of the center of the plastic deformation loops and their width practically do not change with increasing number of cycles, whereas the stress amplitudes can vary depending on the cyclic properties and degree of material damage at a given loading time. Under soft symmetric loading conditions, the coordinates of the center of the plastic deformation loops also does not change and the width of the loops first slightly decreases and then approaches a certain stable value.

A more complex picture of cyclic hysteresis loops is observed under soft asymmetric loading conditions. In this case, as the number of loading cycles increases, the rigid-body displacement of the hysteresis loops is shifted in the direction of the largest amplitude of the strain tensor and the width of the loops changes, with the parameters characterizing these changes asymptotically approaching some stationary values. These features of cyclic deformation occur in the first stage of the damage accumulation process, where the damage developing in the material does not have a significant effect on deformation characteristics. In the subsequent stages of the process, gradual softening of the material takes place and the cyclic deformation pattern becomes even more complicated.

Due to the nonuniformity of the stress-strain state at various points of the material and due to stress and strain redistribution during plastic deformation, a single loading regime rarely occurs during cyclic deformation of real structures.

In this paper, we present the results of a numerical study of the elastoplastic deformation and damage accumulation in structural members of 12Kh18N10T stainless steel under various low-cycle loading conditions using a damaged material model implemented in the UPAKS software [2]. Plastic deformation of the material is modeled using a thermoplasticity model describing the main features of plastic deformation under monotonic and block cyclic loadings and implemented in the UPAKS software [2]. Numerical solution of linearized problems is carried out using the finite element method with isoparametric quadratic finite elements implemented in UPAKS [2].

1. SIMULATION OF LOW-CYCLE LOADING UNDER UNIFORM STRESS-STRAIN CONDITIONS

The elastic-plastic deformation of a thin-walled cylindrical specimen of 12Kh18N10T steel under various cyclic loading conditions is considered. The length of the working part of the specimen is $l = 6.0$ mm, the outer diameter $D = 21.0$ mm, and the wall thickness $h = 1.0$ mm.

Axial loads were applied to the ends of the specimen (displacements in the case of hard loading or distributed loads in the case of soft loading) that change in a cycle according to a given law. The loading process consisted of a sequence of identical cycles, each of which comprised three stages: 1) loading to the maximum positive value; 2) unloading with subsequent loading to negative values; 3) unloading. The numerical solution of the problems was carried out in an axisymmetric formulation using isoparametric finite elements implemented in the UPAKS software with a quadratic distribution of displacement functions.

1.1. Hard Loading

Two loading regimes with the displacements of the ends at the stages U_1, U_2, and U_3 were considered:

— symmetric loading: $U_1 = 0.05$ mm, $U_2 = -0.05$ mm, and $U_3 = 0$;

— asymmetric loading: $U_1 = 0.06$ mm, $U_2 = -0.04$ mm, and $U_3 = 0$.

Figure 1 shows the calculated curves of the axial stresses σ versus axial strains e for the first seven cycles of symmetric loading.

The studies have shown that for the loading conditions considered, the hysteresis loops are stabilized almost after the first cycle. Furthermore, in the case of symmetric loading, the loops are symmetric with respect to the coordinate origin, and in the case of asymmetric loading, they are shifted along the strain axis by an amount equal to the degree of asymmetry of the cycle. The width of the loops does not change and is determined by the amplitude values of the end displacements.

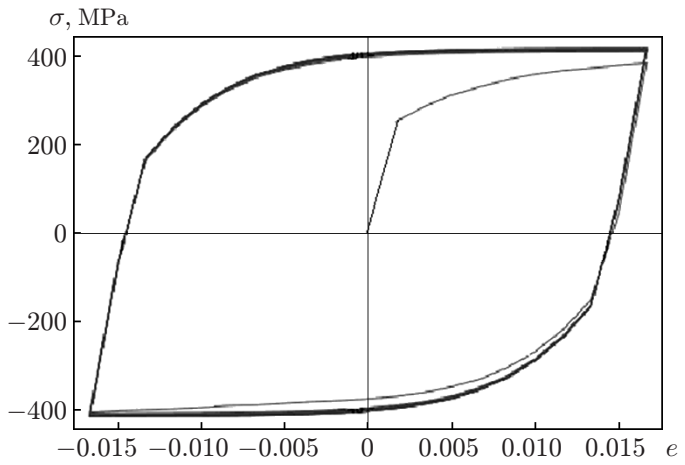

Fig. 1. Axial stress σ versus axial strain e during hard symmetric loading for the first seven cycles.

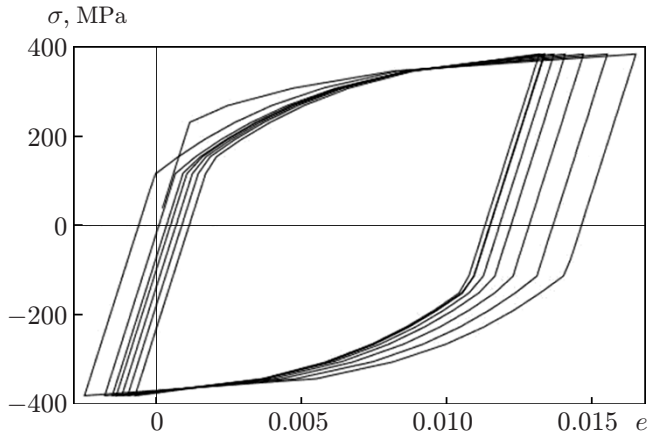

Fig. 2. Axial stresses σ versus axial strains e for the first seven cycles of soft symmetric loading.

1.2. Soft Symmetric Loading

We considered soft symmetric loading with stresses p_1, p_2, and p_3 distributed at the end of the specimen and corresponding to the ends of the three loading stages of the cycle: $p_1 = 385$ MPa, $p_2 = -385$ MPa, and $p_3 = 0$. The calculated curves of the axial stresses σ versus axial strains e for the first seven loading cycles are shown in Fig. 2. It is seen that as the number of cycles increases, the coordinates of the centers of the hysteresis loops practically do not change, while the width of the loops gradually decreases, asymptotically approaching some stationary value, which depends on the amplitude of the end stresses and for this problem is reached in a cycle with $n_c \approx 20$.

1.3. Soft Asymmetric Loading

A number of soft asymmetric loading regimes with a constant maximum tensile stress $p_1 = 385$ MPa and a cycle asymmetry parameter $R_\sigma = (p_1 + p_2)/(2p_1) = 0$; 0.110; 0.188; 0.266; 0.305; 0.344 was considered.The case $R_\sigma = 0$ corresponds to the symmetric loading regime considered above, and the case $R_\sigma = 0.5$ to pulsating loading.

The dependence of the axial stresses σ on the axial strains e for the first 20 cycles of soft asymmetric loading for $R_\sigma = 0.266$ is shown in Fig. 3. It is seen that as the number of cycles increases, the hysteresis loops are gradually shifted relative to the coordinate origin along the strain axis and the width of the loops decreases.

Using the parameter $p(n_c)$ defined as the difference of the plastic strain intensities k_s for the current n_c and the first $n_c = 1$ loading cycles: $p(n_c) = k_s(n_c) - k_s(1)$ as a measure of the shift of the loops, we can write the shift

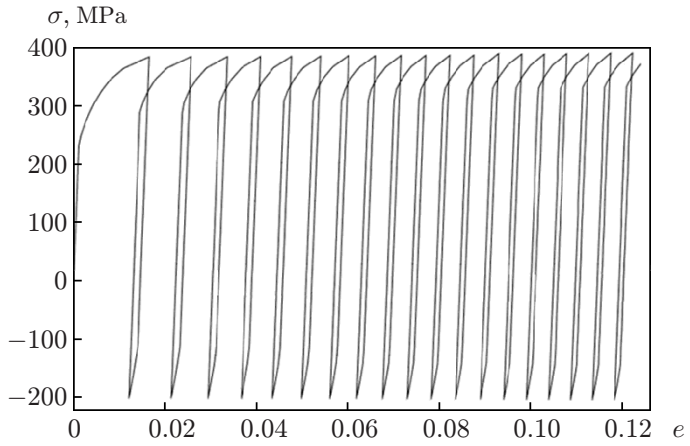

Fig. 3. Axial stresses σ versus axial strains e for the first 20 cycles of soft asymmetric loading ($R_\sigma = 0.266$).

of the loop for one loading cycle as $\Delta p(n_c) = k_s(n_c) - k_s(n_c - 1)$. In this case, the width of the loop is equal to the change in the length of the plastic strain trajectory in one loading cycle: $\Delta k_p(n_c) = k_p(n_c) - k_p(n_c - 1)$, and the deformation amplitude $\Delta e(n_c)$ in one cycle can be defined as the difference between the maximum and minimum axial strains in the cycle: $\Delta e(n_c) = e^{\max} - e^{\min}$.

It follows from Fig. 3 that for $R_\sigma = 0.266$, the functions $\Delta p(n_c)$, $\Delta k_p(n_c)$, and $\Delta e(n_c)$ are monotonic and slowly decreasing.

Similar calculations were also made for other loading conditions. The resulting values of the functions $k_s(n_c)$, $k_p(n_c)$, and $\Delta e(n_c)$ for the first 10 cycles for different values of the cycle asymmetry parameter R_σ are given in Tables 1–3. The function $k_p(n_c)$ increases monotonically with increasing number of cycles, (see Table 2), and during one cycle, it decreases monotonically for all values of R_σ in the investigated range $0 \leqslant R_\sigma < 0.5$. For $R_\sigma = 0.5$, the maximum value of $k_p(n_c)$ is practically reached in the first cycle, and further deformation occurs without accumulation of plastic strain. For values $R_\sigma = 0$; 0.5, the function $k_s(n_c)$ characterizing the plastic strain intensity is practically independent of the number of cycles and reaches the maximum value at the end of the first cycle. For values $0 < R_\sigma < 0.5$, the function $k_s(n_c)$ increases monotonically, and within one cycle, it decreases monotonically. The function $\Delta e(n_c)$ characterizing the strain amplitude in the cycle also decreases monotonically with increasing number of cycles.

From Tables 1–3, it follows that all the functions indicated above depend on the degree of asymmetry of the cycle, and the functions k_p and Δe decrease monotonically with increasing R_σ, and the dependence of the function $k_s(n_c)$ of R_σ is more complex.

Table 4 shows the calculated values of the functions $\Delta p(R_\sigma)$, $\Delta k_p(R_\sigma)$ (change in the length of the plastic strain trajectory), and $\Delta e(R_\sigma)$ for steady-state low-cycle deformation (for the 10-th loading cycle) in the initial stage under the loading conditions considered. For the 10-th loading cycle, the functions $\Delta k_p(R_\sigma)$ and $\Delta e(R_\sigma)$ decrease monotonically, and the function $\Delta p(R_\sigma)$ characterizing the shift of the loop in one cycle reaches the maximum value for $R_\sigma \approx 0.26$.

The above dependences were obtained for cyclic loading with constant values of the maximum tensile stress p_1 and various values of the cycle asymmetry parameter R_σ. Similar calculations were carried out for regimes with a constant stress in the cycle $p_a = p_1 - p_2 = 770$ MPa for a number of positive values of the cycle asymmetry parameter R_σ. It is found that the behavior of the dependences $k_p(n_c)$ and $k_s(n_c)$ is the same as in the above examples.

Thus, features of low-cycle deformation under soft asymmetric loading conditions are the displacement of the hysteresis loops along the strain axis and a decrease in the width of the loops with increasing number of cycles. As the cycle asymmetry parameter increases, the width of the loop and the strain amplitude decrease monotonically in one cycle and the shift of the loops takes a value $\Delta p = 0$ for $R_\sigma = 0$; 0.5 and reaches a maximum in the range $0 < R_\sigma < 0.5$.

Table 1. Dependence $k_s(n_c)$ for the first 10 cycles for different values of the cycle asymmetry parameter R_σ

n_c	k_s					
	$R_\sigma = 0$	$R_\sigma = 0.11$	$R_\sigma = 0.188$	$R_\sigma = 0.266$	$R_\sigma = 0.305$	$R_\sigma = 0.344$
1	0.030 17	0.019 20	0.017 06	0.015 70	0.014 68	0.014 54
2	0.057 97	0.036 85	0.031 08	0.027 02	0.019 46	0.014 66
3	0.083 35	0.053 02	0.043 56	0.037 06	0.023 20	0.014 67
4	0.106 90	0.068 22	0.055 13	0.046 16	0.026 52	0.014 67
5	0.129 30	0.082 80	0.065 92	0.054 64	0.029 62	0.014 67
6	0.150 80	0.096 71	0.076 27	0.062 67	0.031 83	0.014 67
7	0.171 90	0.110 20	0.086 27	0.070 30	0.034 10	0.014 67
10	0.231 90	0.148 80	0.114 90	0.091 79	0.039 95	0.014 67

Table 2. Dependence $k_p(n_c)$ for the first 10 cycles for different values of the cycle asymmetry parameter R_σ

n_c	k_p					
	$R_\sigma = 0$	$R_\sigma = 0.11$	$R_\sigma = 0.188$	$R_\sigma = 0.266$	$R_\sigma = 0.305$	$R_\sigma = 0.344$
1	0.030 17	0.019 20	0.017 06	0.015 70	0.014 68	0.014 54
2	0.057 97	0.036 85	0.031 08	0.027 02	0.019 46	0.014 66
3	0.083 35	0.053 02	0.043 56	0.037 06	0.023 20	0.014 67
4	0.106 90	0.068 22	0.055 13	0.046 16	0.026 52	0.014 67
5	0.129 30	0.082 80	0.065 92	0.054 64	0.029 62	0.014 67
6	0.150 80	0.096 71	0.076 27	0.062 67	0.031 83	0.014 67
7	0.171 90	0.110 20	0.086 27	0.070 30	0.034 10	0.014 67
10	0.231 90	0.148 80	0.114 90	0.091 79	0.039 95	0.014 67

Table 3. Dependence $\Delta e(n_c)$ for the first 10 cycles for different values of the cycle asymmetry parameter R_σ

n_c	Δe				
	$R_\sigma = 0$	$R_\sigma = 0.11$	$R_\sigma = 0.188$	$R_\sigma = 0.266$	$R_\sigma = 0.305$
1	0.019 26	0.008 00	0.005 56	0.003 91	0.002 60
2	0.017 34	0.007 80	0.005 40	0.003 83	0.002 57
3	0.016 16	0.007 64	0.005 30	0.003 77	0.002 56
4	0.015 35	0.007 52	0.005 21	0.003 71	0.002 55
5	0.014 80	0.007 42	0.005 14	0.003 68	0.002 53
6	0.014 39	0.007 31	0.005 09	0.003 64	0.002 52
7	0.014 15	0.007 24	0.005 04	0.003 61	0.002 52
10	0.013 50	0.007 08	0.004 93	0.003 57	0.002 51

Table 4. Functions $\Delta p(R_\sigma)$, $\Delta k_p(R_\sigma)$ and $\Delta e(R_\sigma)$ versus the cycle asymmetry parameter R_σ

R_σ	Δp	Δk_p	Δe	R_σ	Δp	Δk_p	Δe
0	0	0.2000	0.1350	0.266	0.0530	0.0694	0.0357
0.058	0.0413	0.1570	0.0931	0.305	0.0457	0.0538	0.0301
0.110	0.0510	0.1260	0.0708	0.344	0.0168	0.0180	0.0251
0.188	0.0539	0.0920	0.0493	0.500	0	0	0.0188

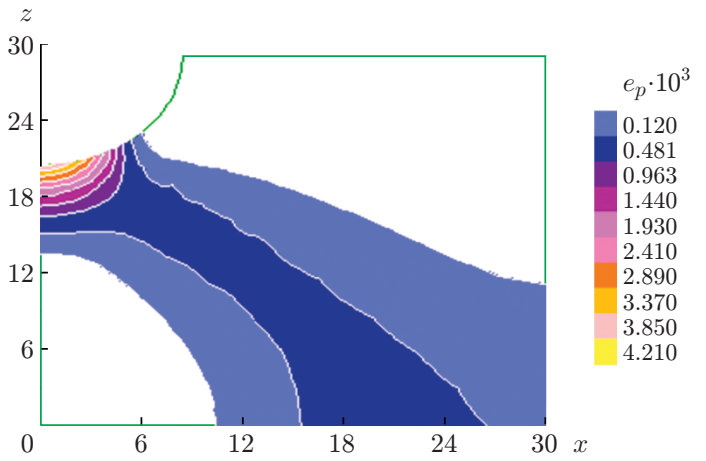

Fig. 4. Plastic strain distribution in the longitudinal section of a cylindrical specimen with a notch cut at the end of the first cycle under hard symmetric loading.

2. SIMULATION OF LOW-CYCLE LOADING UNDER NON-UNIFORM STRESS-STRAIN CONDITIONS

The low-cycle loading of a cylindrical specimen whose working part has a notch cut of radius $R = 8.5$ mm was studied by numerical simulation. The diameter of the working piece of the specimen is 29 mm, and the length of the working part is $L = 30$ mm. The specimen is made of 12Kh18N10T stainless steel and the material functions necessary for the calculations (as well as in the problem considered in Sec. **1**) are constructed on the basis of the experimental data given in [2].

The specimen was uniformly heated to a temperature $T = 350$ °C and subjected to cyclic loading, which, depending of the loading conditions considered, involved either shifts of the ends (hard loading) or loads distributed at the ends of the load (soft loading) varying in the cycle according to a given law.

The numerical solution of the problems was carried out in an axisymmetric formulation using isoparametric finite elements with a quadratic distribution of displacement functions.

The following cyclic loading conditions were considered:

— hard symmetric loading with a shift of the ends at the stages $U_1 = 0.0413$ mm, $U_2 = -0.0413$ mm, and $U_3 = 0$;

— soft symmetric loading with the stresses p_1, p_2, and p_3 distributed at the end of the specimen for three loading stages of the cycle: $p_1 = 19.7$ MPa, $p_2 = -19.7$ MPa, and $p_3 = 0$;

— soft asymmetric loading: $p_1 = 19.7$ MPa, $p_2 = -10.0$ MPa, and $p_3 = 0$.

Figure 4 shows the plastic strain in the longitudinal section of the specimen in the first cycle of hard symmetric loading.

In the numerical simulation, we controlled the stress–strain state and the degree of material damage in the most heavily loaded point of the specimen located in the outer fibers of the central cross section.

It was established that in the first stage of the process (initial stage of damage accumulation) under symmetric loading (both hard and soft), the cyclic deformation process at the point considered is slightly different from deformation under uniform stress-strain conditions. In the case of asymmetric cycles, the deformation process differs from deformation under uniform stress-strain conditions in that the loops are gradually shifted in the direction of negative stresses, with the shift increasing with increasing degree of material damage.

3. DAMAGE DEVELOPMENT UNDER SOFT ASYMMETRIC LOADING

Under hard symmetric and asymmetric loading conditions, the damage accumulation process and low-cycle fracture of structural material are fairly accurately described by the models used in this paper, and the obtained results are in good agreement with experimental data. Figure 5 shows an experimental low-cycle fatigue curve for 12Kh18N10T steel (curve *1*) and a curve constructed using fatigue calculation results (curve *2*) for the spec-

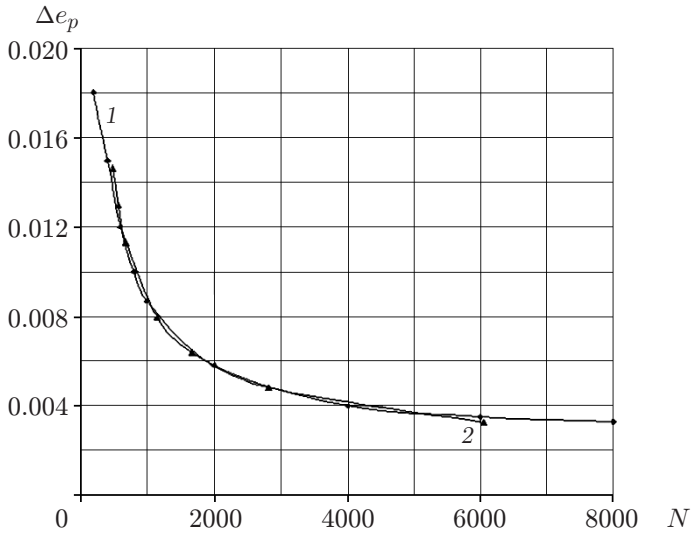

Fig. 5. Experimental (*1*) and calculated (*2*) low-cycle fatigue curves of a notched cylindrical specimen under hard symmetric loading.

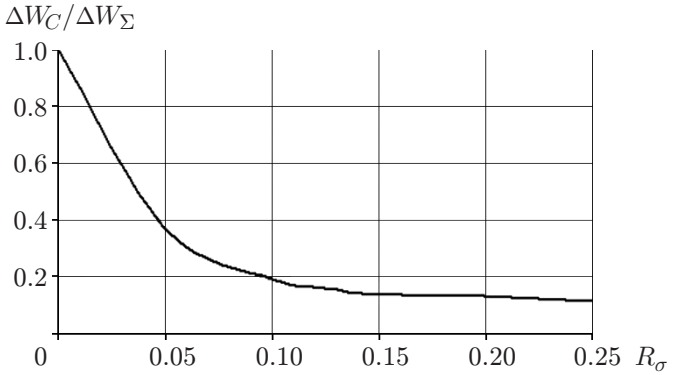

Fig. 6. Ratio of the cyclical component of the energy ΔW_C to its total value ΔW_Σ in the loading cycle versus the asymmetry parameter R_σ under soft asymmetric loading conditions.

imen considered in Subsection 1.1 under hard symmetric loading for different plastic strain amplitudes in the range $\Delta e_p = 0.003\,26$–$0.014\,66$.

As shown above, under soft asymmetric loading conditions, plastic strains can have a significant contribution to the irreversible strain accumulated in the material. In this case, the energy of plastic loosening W_S, which determines the material fracture in the loading portion corresponding to the quasistatic process, can be comparable to and even exceed the energy W_C corresponding to the cyclic process. Figure 6 shows a curve of the ratio of the cyclic component of the energy ΔW_C to its total value ΔW_Σ in the loading cycle versus the cycle asymmetry parameter R_σ for the loading conditions considered in Subsection 1.3. It can be seen that for $R_\sigma \geqslant 0.2$, the quasi-static component of the energy increment in one cycle can amount to more 80% of the total energy increment ΔW_Σ.

According to the damage accumulation model used in the present study, the change in the damage function in the material in the elementary loading step is defined as the ratio of the current change in the energy of plastic loosening ΔW to the maximum value of this energy for the type of fracture W^R considered in the study. If, for quasi-static and cyclic processes, the energies W^R are assumed to be the same, these processes may not be distinguished and the change in the damage function can be calculated based on the general scheme. However, the maximum energy W_S^R for quasi-static processes and W_C^R for cyclic processes may differ from each other, the more

so as these energies are determined in different types of experiments. Therefore, the energies W_S^R and W_C^R can generally be assumed to be independent of each other, and we can determine the changes in the damage functions for quasi-static ($\Delta\psi_S$) and cyclic ($\Delta\psi_C$) processes independently and then calculate the corresponding changes in the damage measures $\Delta\omega_S$ and $\Delta\omega_C$ (ω is the measure of the reduction in the effective cross-sectional area relative to the cross-sectional area in the initial state (for undamaged material $\omega = 0$ for completely damaged material $\omega = 1$) [2, 3]).

To determine the value of the function W_C^R for a given temperature, it is sufficient to use one point in the low-cycle fatigue curve plotted for hard symmetric loading at this temperature. To determine the function of W_S^R, it is necessary to numerically simulate the fracture of the specimen under uniaxial tension with large strain and necking taken into account. This should be done so as to obtain the agreement between the calculated and experimental results. Due to the significant nonuniformity of the stress-strain state of the specimen in the fracture zone, the error in determining the function W_S^R based on the this approach can be rather large. This function can be determined more accurately using the results of low-cycle fatigue tests under soft asymmetric loading. In this case, the cycle asymmetry parameter should be chosen such that it is possible to determine the quasi-static component of the energy fracture for the minimum plastic strain accumulated by the time of fracture. For the above example, we can set $R_\sigma \approx 0.1$.

To implement this combined model describing the elastoplastic damage accumulation under various conditions of variable loading, it is necessary to separately calculate the changes in the energies ΔW_S and ΔW_C in the elementary loading step and the corresponding changes in the damage functions $\Delta\psi_S$ and $\Delta\psi_C$ for quasi-static and cyclic loadings using the relations

$$\Delta W_S = \rho_{ij}\Delta e_{ij}^p, \quad k_s - k_s^{\max} > 0, \qquad \Delta W_C = \rho_{ij}\Delta e_{ij}^p, \quad k_s - k_s^{\max} \leqslant 0,$$
$$\Delta\psi_S = \Delta W_S / W_S^R(\Pi), \qquad \Delta\psi_C = \Delta W_C / W_C^R(\Pi),$$

where k_s and $k_s^{\max}$ are the current and previous maximum intensity plastic strains at each point in the material.

If we set $W_S^R = W_C^R$, the proposed model is transformed into the basic version of the model [2].

CONCLUSIONS

Deformation and damage accumulation in structural materials under different low-cycle loading was studied by numerical simulation in the initial stage of the process where the damage developing in the material has no significant effect on deformation characteristics. The main features of plastic deformation and damage in materials for different low-cycle loading conditions (hard, soft, symmetric and asymmetric) and parameters characterizing the asymmetry of cycles were determined. The results can be used to refine damage accumulation models for arbitrary quasi-static and cyclic loads.

This work was supported by the Russian Sciences Foundation (Grant No. 16-19-10237).

REFERENCES

1. O. I. Bekh and Yu.G. Korotkikh, "Equations of Damage Mechanics for Cyclic Non-Isothermal Deformation of Materials," in *Applied Problems of Strength and Plasticity: Methods of Solution* (Gork. Gos. Univ., Gorkii, 1989), pp. 28–37 [in Russian].
2. D. A. Kazakov, S. A. Kapustin , and Yu. G. Korotkikh, *Modeling of Deformation and Fracture of Materials and Structures* (Nizhegor. Gos. Univ., Nizhny Novgorod, 1999) [in Russian].
3. I. A. Volkov and Yu. G. Korotkikh, *Equations of State of Damaged Viscoelastoplastic Media* (Fizmatlit, Moscow, 2008) [in Russian].
4. J.-L. Chaboche, P. Kanoute, and F. Azzouz, "Cyclic Inelastic Constitutive Equations and Their Impact on the Fatigue Life Predictions," Intern. J. Plasticity **35**, 44–66 (2012).
5. V. S. Bondar, V. V. Danshinand, and A. A. Kondratenko, "Version of the Theory of Thermoplasticity," Vetsn. Perm. Nats. Issled. Politekhn. Univ. Mekhanika, No. 2, 21–35 (2015).
6. S. A. Kapustin, V. A. Gorokhov, and Yu. A. Churilov, "Algorithms for Predicting the Low-Cycle Strength of Structures Based on the Finite Element Method," Probl. Prochn. Plastichn. **73**, 13–24 (2011).